Dielectronic recombination of Pb^{79+} atomic ions at high spectral resolution

D. M. Mitnik and M. S. Pindzola
Department of Physics, Auburn University, Auburn, Alabama 36849

N. R. Badnell
Department of Physics and Applied Physics, University of Strathclyde, Glasgow G4 0NG, United Kingdom
(Received 24 August 1999; published 6 January 2000)

Dielectronic recombination cross sections for $\Delta n=0$ transitions in Pb^{79+} are calculated in a fully relativistic distorted-wave approximation. We present detailed nlj results for the first resonances associated with the $2s \rightarrow 2\bar{p}$ $(j=\frac{1}{2})$ core excitation, which opens up at $n=20$, and for the first resonances associated with the $2s \rightarrow 2p$ $(j=\frac{3}{2})$ core excitation, which overlap the $1s^2 2\bar{p}nl$ resonances series. An accurate identification of these peaks is of importance in the ongoing dielectronic recombination experiments for the determination of the $2s$-$2p$ threshold energies. Careful examinations of Breit interaction and QED effects are performed in order to calculate the resonance energies with a resolution comparable with present experimental resolution. Fully relativistic calculations for Auger and radiative rates are performed for an accurate determination of the peak heights.

PACS number(s): 34.80.Lx

I. INTRODUCTION

Dielectronic recombination (DR) plays a fundamental role in the determination of the level populations and ionization balance of high-temperature non-LTE laboratory and astrophysical plasmas. The development of ion accelerators, traps, and storage rings has made possible the observation of increasingly more detailed and complex DR spectra. The high resolution achieved in the current experiments, at the order of 10–100 meV [1,2] in light ions, has challenged the most sophisticated theoretical computations for interpretation [3,4].

In addition to its application in astrophysics and fusion plasmas, DR provides a unique tool for precision spectroscopy of intermediate double excited states. In particular, with the capability of the storing and cooling of even the heaviest highly charged ions, the experimental assessment of influences from relativistic and QED effects is now possible. For example, the $1s^2 2p_{1/2}nl$ resonances on the DR spectra of the heaviest Li-like ions consist of a series of peaks, which can be assigned to different principal n quantum numbers. The extrapolation to $n=\infty$ allows the indirect determination of the $2p_{1/2}$-$2s_{1/2}$ Lamb shift in nonhydrogenic systems.

Previous DR calculations on heavy highly charged Li-like ions were performed on Au^{76+}, Bi^{80+}, and U^{89+} [5–8]. All these calculations demonstrated that the effect of relativity can change the peak positions, as well as the peak heights, therefore the relativistic effects should be included in calculations of DR cross sections in heavy highly ionized ions. To compare with early low-resolution experimental measurements, the convoluted peaks in the theoretical spectra correspond to resonances from each n principal quantum number. The purpose of this work is to present a convoluted spectrum at much higher resolution coming from individual nlj resonances. In the paragraphs below, we present the results of relativistic calculations of the first peaks of the $1s^2 2p_{1/2}nl$ and $1s^2 2p_{3/2}nl$ series of the DR spectra of Pb^{79+}. We focus our study on the $1s^2 2p_{1/2}20l$ resonances, which are located between 14 and 18 eV. These are the first set of nlj resonances that need to be identified in the experimental spectrum, so that, by extrapolation on the principal quantum number n, the threshold energy of the series can be obtained. We also perform fully relativistic calculations of the $1s^2 2p_{3/2}6l$ resonances. These large peaks cover an energy range of about 300 eV, and overlap the $1s^2 2p_{1/2}nl$ resonance series.

In Sec. II we describe the theoretical methods used in the calculations, in Sec. III we compare the results of the calculations using different methods, and, finally, the results are summarized in Sec. IV.

II. THEORY

In the isolated-resonance and independent-processes approximation, the dielectronic recombination cross section for a given initial level i through an intermediate level j is given (in atomic units) by [9]

$$\sigma(i\rightarrow j)=S(i\rightarrow j)\frac{(\Gamma_j/2\pi)}{(E-E_c)^2+\Gamma_j^2/4} \tag{1}$$

where the width of the resonance j is given by

$$\Gamma_j=\sum_m A_a(j\rightarrow m)+\sum_n A_r(j\rightarrow n) \tag{2}$$

and the DR strength is expressed as

$$S(i\rightarrow j)=\frac{\pi^2}{E_c}\frac{g_j}{2g_i}A_a(j\rightarrow i)\left[\frac{\sum_k A_r(j\rightarrow k)}{\Gamma_j}\right]. \tag{3}$$

Here E_c is the energy of the continuum electron, which is fixed by the position of the resonance j, g_j is the statistical weight of the $(N+1)$-electron ion doubly excited level, g_i is

 ©2000 The American Physical Society

the statistical weight of the N-electron ion initial target level, $A_a(j\rightarrow m)$ is the autoionizing rate from level j to level m, and $A_r(j\rightarrow k)$ is the radiative rate from level j to any lower energy level k. The term in the square brackets in Eq. (3) is the branching ratio for radiative stabilization.

For the calculation of the full $2s\rightarrow 2\overline{p}$ core transition DR spectra at relatively low (1–10 eV) resolution, the AUTOSTRUCTURE code [10,11] has been used. For application to highly charged ions, this code generates the bound orbital functions using a semirelativistic procedure, following the work of Cowan and Griffin [12], in which the mass velocity and Darwin operators have been added to the nonrelativistic Hartree-Fock differential equations. Perturbation theory is then used to evaluate the remaining one-body and two-body fine-structure interactions.

For a high-resolution spectrum, a fully relativistic method is needed. We first use a relativistic, parametric potential approximation [13] to the solution of the Dirac Hamiltonian, implemented in the HULLAC package [14]. The main idea of the parametric potential method is the introduction of a central potential as an analytic function of screening parameters which are determined by minimizing the first-order relativistic energy of a set of configurations. This optimized potential is used to calculate all one-electron orbitals and energies, relativistic multiconfiguration bound states and their energies, continuum orbitals, and all the required transition rates. The first-order perturbations theory contributions from the Breit interaction and QED corrections to the energies are also included in the calculations.

In order to calculate the threshold energies more accurately, we also use the atomic structure codes of Grant *et al.* [15], based on the multiconfiguration Dirac-Fock (MCDF) approximation [16]. Energies and bound-state wave functions are obtained using Grant's MCDF code, which includes nuclear size effects, Breit interactions, and QED corrections.

The various A_a and A_r rates entering Eq. (1) are calculated using first-order perturbation theory. All the methods use the distorted-wave approximation for the continuum wave functions, which is extremely accurate for highly charged ions. The fully relativistic calculations include both Coulomb electrostatic and Breit electromagnetic contributions to the autoionizing transition amplitudes. AUTOSTRUCTURE and HULLAC codes generate the rates as well as the atomic structure. In order to generate the rates using the MCDF codes, a method described in Ref. [6] is used, implemented in what we call the DR/MCDF package.

III. RESULTS

The reactions we consider for Pb^{79+} are

$$Pb^{79+}(1s^22s)+e^-\rightleftharpoons Pb^{78+}(1s^22\overline{p}nl)\rightarrow\begin{cases}Pb^{78+}(1s^22snl)+h\nu_1\\ Pb^{78+}(1s^22\overline{p}n'l')+h\nu_2\end{cases} \tag{4}$$

for $n\geqslant 20$, $n'<20$, and $l'<n'$, and also

$$Pb^{79+}(1s^22s)+e^-\rightleftharpoons Pb^{78+}(1s^22pnl)\rightarrow\begin{cases}Pb^{78+}(1s^22snl)+h\nu_3\\ Pb^{78+}(1s^22pn'l')+h\nu_4\end{cases}$$
$$\updownarrow$$
$$Pb^{79+}(1s^22\overline{p})+e^- \tag{5}$$

for $n\geqslant 6$, $n'<6$, and $l'<n'$.

In Fig. 1 we show the results of the $1s^22s_{1/2}$ and $1s^22p_{1/2}$ energy levels calculated by using the MCDF code. The figure shows the zeroth-order Dirac-Fock energy, the first-order perturbation theory contribution of the Breit interaction, and the hydrogenic vacuum polarization and self-energy screening corrections. The total contribution of the last two corrections is marked as ''QED.'' The calculated total energy difference between the $1s^22s_{1/2}$ and $1s^22p_{1/2}$ levels is 231.2 eV, which agrees very well with the results obtained by Kim *et al.* [17], 230.8 eV. For the same energy calculation, but without including QED effects, we obtained 258.7 eV, which also agrees with Kim *et al.*'s results, 258.8 eV. The calculated total energy difference between the $1s^22s_{1/2}$ and $1s^22p_{3/2}$ levels is 2642.4 eV, in agreement with Kim *et al.*, who obtained 2642.0 eV. The same calculations without QED effects give 2667.3 eV (Kim *et al.* obtained 2667.3 eV). Figure 1 also shows the results of the zeroth-order Dirac-parametric energies calculated by using the HULLAC code (including QED effects). For the $1s^22s_{1/2}$-$1s^22p_{1/2}$ transition, we calculate an energy of 242.8 eV, and for the $1s^22s_{1/2}$-$1s^22p_{3/2}$ transition, the energy is 2651.9 eV.

In order to provide a general overview of the low-energy region of the DR spectra of Pb^{79+}, we present in Fig. 2 the semirelativistic results of the DR cross section from AUTOSTRUCTURE in the 0–300 eV energy range. The DR cross sections have been convoluted with a 3 eV full width at half maximum (FWHM) Gaussian. This spectrum consists of a series of peaks, belonging to the $1s^22p_{1/2}nl$ resonances, which starts at $n=20$. The threshold energy of this Rydberg series resides at 230 eV. This threshold is not visible in the figure because we limit our calculations to $n\leqslant 50$. However, the resonances for very high n would not be noticeable due to the presence of some peaks belonging to the $1s^22p_{3/2}6l$

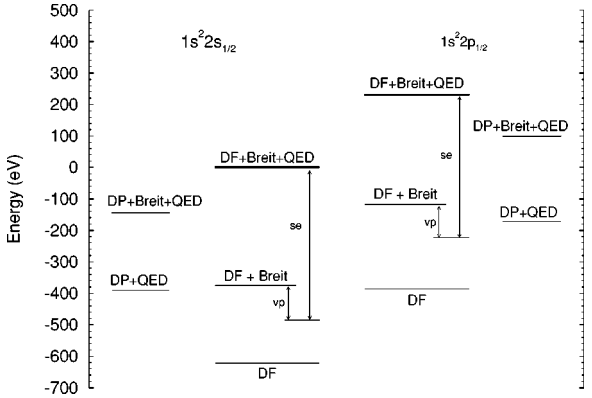

FIG. 1. Relative energies of the $1s^22s$ and $1s^22p_{1/2}$ levels for the Pb^{79+} ion, calculated by using the MCDF method, implemented in Grant's code. The figure shows the zeroth-order Dirac-Fock energy (DF), the first-order perturbation theory contribution of the Breit interaction energy, the vacuum polarization correction (vp), and the self-energy screening correction to the energy (se). The total contribution of the last two corrections is marked as ''QED'' corrections. The small lines at the sides of the figures show the zeroth-order plus QED and zeroth-order plus Breit interaction plus QED energies, calculated by using the parametric potential method for the solution of the Dirac Hamiltonian (DP).

resonances in the same energy range. The energy results of these calculations have been adjusted (separately for each series) in order to match the threshold energies with those obtained from the fully relativistic MCDF calculation, including Breit and QED corrections. Thus, we shifted the position of the peaks -155 eV for the $2s$-$2\overline{p}$ series and -166 eV for the $2s$-$2p$ series.

The aim of this work is to provide a high-resolution DR spectrum which includes detailed structure within the n peaks. Therefore, we need to go beyond the semirelativistic approximation, and perform a fully relativistic calculation. For an accurate determination of the strength of the peaks, the Breit interaction in calculations of Auger rates is also

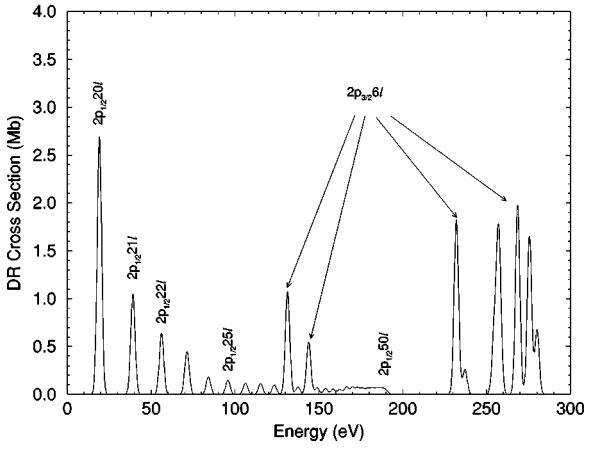

FIG. 2. Dielectronic recombination cross sections for the Pb^{79+} ion, through the $1s^22p_{1/2}nl$ ($n=20-50$) and $1s^22p_{3/2}6l$ intermediate autoionizing levels. The DR cross sections have been obtained by using the semirelativistic AUTOSTRUCTURE code, and have been convoluted with a 3 eV full width at half maximum Gaussian.

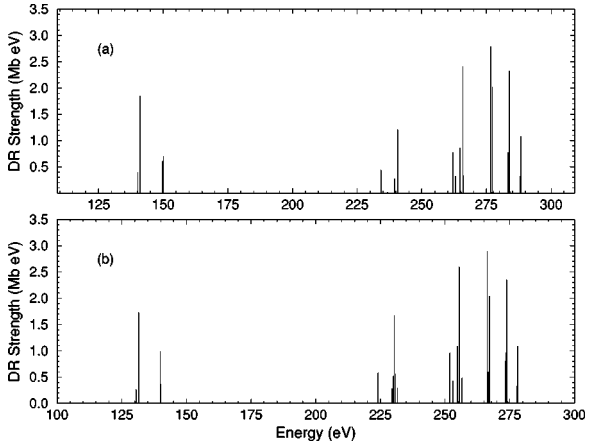

FIG. 3. Dielectronic recombination strengths through the $1s^22p_{3/2}6l$ levels for the Pb^{79+} ion. Part (a) shows the results obtained by using the HULLAC code, and part (b) shows the results obtained by using the DR/MCDF code.

included. Figure 3 shows the $1s^22p_{3/2}6l$ DR strengths, obtained by using the HULLAC code, and the DR/MCDF code. We present the results in terms of strengths, since the natural linewidths of the resonances are not visible in this scale. The comparison between the two calculations shows very good agreement. In order to facilitate the comparison, the energy axis of the HULLAC results was shifted toward the lower energies, by 9 eV. As shown in Fig. 1, the absolute energies calculated by using the MCDF and HULLAC codes differ by approximately 200 eV. However, as shown in Fig. 3, the relative energies calculated by using the parametric potential method are still very accurate. The main difference in the calculational methods is that MCDF optimizes the calculation on the separate configurations, and HULLAC utilizes the same potential for all the configurations, providing accurate relative energies. The resonances gather in pairs of jj subconfigurations, i.e., $2p_{3/2}6l_{j=l+1/2}$ and $2p_{3/2}6(l+1)_{j=l+1-1/2}$. Inside each one of these groups, there is a dominant resonance, and it corresponds to a level having a total J value equal to $J=|3/2+j|$. The dominant transition in the whole manifold (at 273.7 eV) corresponds to the $1s^22p_{3/2}6f_{7/2}$ ($J=5$) level.

Figure 4 shows the $1s^22p_{1/2}20l$ DR cross section, obtained by using the DR/MCDF code. We have been able to use this code for detailed calculations until $l=5$, including the core radiative transitions between $1s^22p_{1/2}20l$ to $1s^22s_{1/2}20l$ levels. For highly excited ions, the radiative transition rates are, in general, much higher than the autoionizing rates. Therefore, the DR cross section becomes roughly proportional to the autoionization rates [see Eq. (1)]. The autoionizing rates are decreasing as the l quantum number increases, and in consequence, it seems possible to neglect the DR contribution from levels having high-l quantum angular numbers. However, these levels have a small quantum defect, and the convoluted cross section is not negligible due to the accumulation of many resonances in a narrow energy range. Therefore, we include the contribution of the $1s^22p_{1/2}20l$ ($l>5$) by invoking the following procedure. First, we calculate the autoionization rates by using the

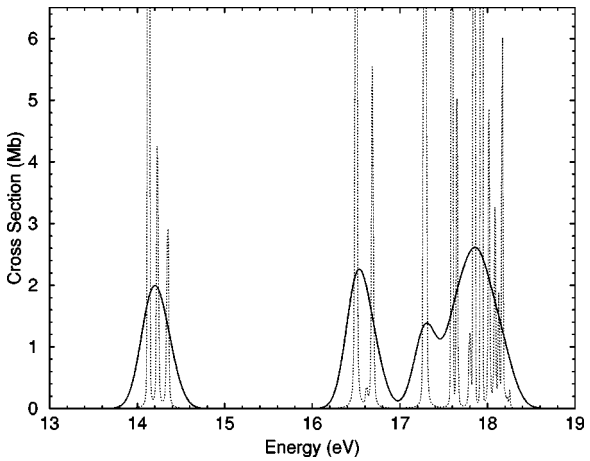

FIG. 4. Dielectronic recombination cross sections through the $1s^2 2p_{1/2} 20l$ levels for the Pb^{79+} ion. The DR cross sections have been obtained by using the DR/MCDF code. The dashed line shows the natural linewidth of the DR cross-section resonances. The solid line results have been convoluted with a 0.3 eV full width at half maximum Gaussian.

AUTOSTRUCTURE code, for all the levels belonging to the $1s^2 2p_{1/2} 20l$ configurations. Although the low-l autoionization rates from our fully relativistic calculations differ substantially from the semirelativistic calculation, by $l=5$ there is reasonable agreement between the two approximations. Therefore, we include the AUTOSTRUCTURE results for the autoionization rates for the rest of the levels of the $1s^2 2p_{1/2} 20l$ $(l>5)$ configurations. Second, the energies have been calculated using a relativistic hydrogenic approximation. As the l-quantum number increases, the levels become more degenerate, and the energies of the levels are roughly a function of only the j-quantum number of the valence electron. Finally, an additional approximation is needed for the calculation of the radiative transitions involving the valence electron, i.e., from $1s^2 2p_{1/2} 20l$ to $1s^2 2p_{1/2} n'l'$. Since the energy difference between the $2p_{1/2}$-$2s_{1/2}$ is relatively small, the corresponding core radiative transition is quite small. Therefore, the transitions involving the valence electron become the dominant radiative path. To handle the high Rydberg states involved, we calculate these transitions by using analytic expressions for the dipole length integrals, based on analytic expressions for the Coulomb functions, as detailed by Burgess *et al.* in Ref. [18]. The DR cross sections of Fig. 4 show details of the autoionizing double excited states at the level of natural linewidths, and also provide details of the nlj structure of the configurations. Figure 4 also shows the DR cross sections convoluted with a 0.3 full width at half maximum (FWHM) Gaussian, in order to provide comparisons with possible experimental measurements. Besides the first three peaks in the spectrum, corresponding to the $1s^2 2p_{1/2} 20s$ and $1s^2 2p_{1/2} 20p$ resonances, each different $2p20l$ configuration contributes two peaks to the DR spectrum, one corresponding to a pair of levels having $J=l-1$ and $J=l$, and the other corresponding to the pair of levels with $J=l$ and $J=l+1$. The dominant resonances at 14.14 eV, 16.51 eV, 17.85 eV, and 17.94 eV correspond to the $2p20s_{1/2}$ $(J=1)$, $2p20p_{3/2}$ $(J=1$ and $J=2)$, $2p20g_{7/2}$ $(J=4)$, and $2p20h_{11/2}$ $(J=5)$ intermediate levels, respectively.

IV. SUMMARY

In this work we have calculated the dielectronic recombination cross sections for Pb^{79+}. The high resolution achieved in current experiments requires the presentation of the theoretical results detailed at the level of natural linewidths. In particular, for highly ionized heavy ions, fully relativistic calculations are needed. For an accurate determination of the position of the resonances in the DR spectra, careful examination of Breit and QED effects has been performed. For the calculation of the heights of the peaks, fully relativistic Auger and radiative rates have been computed. We look forward to an experimental determination of the cross sections presented here.

ACKNOWLEDGMENTS

We would like to thank Professor Alfred Müller for discussions about ongoing experiments at GSI. This work was supported in part by the U.S. Department of Energy under Grant No. DE-FG05-96ER54348 with Auburn University, and under Grant No. DE-GC02-91-ER75678 with Alabama EPSCOR.

[1] S. Mannervik, D. DeWitt, L. Engström, J. Lidberg, E. Lindroth, R. Schuch, and W. Zong, Phys. Rev. Lett. **81**, 313 (1998).

[2] A. Müller, T. Bartsch, C. Brandau, G. Gwinner, A. Hoffknecht, C. Kozhuharov, A. A. Saghiri, S. Schippers, M. Schmitt, and A. Wolf, *Atomic Processes in Plasmas*, Proceedings of the 11th APS Topical Conference, Auburn, AL, edited by E. Oks and M.S. Pindzola (AIP Press, New York, 1998), p. 241.

[3] *Recombination of Atomic Ions*, edited by W.G. Graham, W. Fritsch, Y. Hahn, and J.A. Tanis, Vol. 296 of *NATO Advanced Study Institute Series B: Physics* (Plenum Press, New York, 1992).

[4] Second Euroconference on Atomic Physics with Stored Highly Charged Ions, edited by R. Schuch, E. Lindroth, and H. Jürgen Kluge [Hyperfine Interact. **108**, 149 (1997)].

[5] M.H. Chen, Phys. Rev. A **41**, 4102 (1990).

[6] M.S. Pindzola and N.R. Badnell, Phys. Rev. A **42**, 6526 (1990).

[7] N.R. Badnell and M.S. Pindzola, Phys. Rev. A **43**, 570 (1991).

[8] W. Spies, A. Müller, J. Linkemann, A. Frank, M. Wagner, C. Kozhuharov, B. Franzke, K. Beckert, F. Bosch, H. Eickhoff, M. Jung, O. Klepper, W. König, P.H. Mockler, R. Moshammer, F. Nolden, U. Schaaf, P. Spädtke, M. Steck, P. Zimmerer, N. Grün, W. Scheid, M.S. Pindzola, and N.R. Badnell, Phys. Rev. Lett. **69**, 2768 (1992).

[9] Y. Hahn, Adv. At. Mol. Phys. **21**, 123 (1985).
[10] N.R. Badnell, J. Phys. B **19**, 3827 (1986).
[11] N.R. Badnell and M.S. Pindzola, Phys. Rev. A **39**, 1685 (1989).
[12] R.D. Cowan and D.C. Griffin, J. Opt. Soc. Am. **66**, 1010 (1976).
[13] M. Klapisch, Comput. Phys. Commun. **2**, 239 (1971).
[14] J. Oreg, W.H. Goldstein, M. Klapisch, and A. Bar-Shalom, Phys. Rev. A **44**, 1750 (1991).
[15] I.P. Grant, B.J. McKenzie, P.H. Norrington, D.F. Mayers, and N.C. Pyper, Comput. Phys. Commun. **21**, 207 (1980).
[16] I.P. Grant and H.M. Quiney, Adv. At. Mol. Phys. **23**, 37 (1988).
[17] Y.-K. Kim, D.H. Baik, and P. Indelicato, Phys. Rev. A **44**, 148 (1991).
[18] A. Burgess, D.G. Hummer, and J.A. Tully, Philos. Trans. R. Soc. London, Ser. A **266**, 255 (1970).